Very High Cycle Fatigue Strength of a High Strength Steel under Sea Water Corrosion

Thierry PALIN-LUC[1)*], Claude BATHIAS[2)]

[1)] Arts et Metiers ParisTech, I2M, UMR CNRS, Universite Bordeaux 1,
Esplanade des Arts et Metiers, 33405 Talence Cedex, France
[2)] Universite Paris X, LEME, 50 rue de Sevres, 92410 Ville d'Avray, France
*Corresponding author: thierry.palin-luc@ensam.eu

Abstract The effect of sea water corrosion on the gigacycle fatigue strength of a martensitic-bainitic hot rolled steel used for producing off-shore mooring chains for petroleum platforms was studied. Three different environments and conditions: (i) air; (ii) air after pre-corrosion, (iii) air under real time artificial sea water flow (in situ) were considered for testing smooth specimens under fully reversed tension between 10^6 and 10^{10} cycles. A drastic effect of corrosion was observed. For the fatigue life greater than 10^8 cycles, the fatigue strength is reduced by a factor more than 5 compared with non corroded specimens (virgin). Corrosion pits due to pre-corrosion, if any, or pits resulting from corrosion in real time during cyclic loading are the crack initiation sites. The calculation of the mode I stress intensity factor at hemispherical surface defects (pits) combined with the Paris-Hertzberg-Mc Clintock crack growth rate model showed that the fatigue crack initiation regime represents most of the fatigue life in the VHCF regime. Original additional experiments shew physical evidences that the fatigue strength in the gigacycle domain under sea water flow is mainly governed by the corrosion process with a strong coupling between cyclic loading and corrosion.

Keywords Gigacycle fatigue, corrosion, steel, crack initiation, crack growth

1. Introduction

Mooring chains for off-shore petroleum platforms are loaded in VHCF regime and in sea water environment. They are designed for 30 years that is around 10^9 cycles because of the ocean waves 24 hours a day. The aim of this study is to study the gigacycle fatigue strength of the low-alloy steel used for manufacturing such chains and the effects on this strength of both pre-corrosion and corrosion in sea water environment. Many studies carried out on steel and aluminum alloys in the gigacycle regime have demonstrated that there is not a fatigue limit for such metals beyond 10^7 cycles as was believed in the past [1, 2]. It has been shown that fatigue cracks initiate mainly at surface defects in the short fatigue life regime, but may shift to subsurface in the long life range [3]. Other studies have shown that defects like non-metallic inclusions, pores [4] or pits [5 - 7] are the key factors, which control the fatigue properties of metals in very high cycle fatigue (VHCF). Furthermore, in some works it has been proven that crack initiation dominates the total fatigue life of specimens in gigacycle fatigue [8, 9]. On the other hand, the influence of static deformation has been studied confirming that both passive and transpassive current densities on stainless steel reach a maximum in the course of growing plastic strain [10]. Other works have investigated the dissolution of chemical products in stainless steel with active, passive and intermediate potentials where it is presumed that dissolution is enhanced during cyclic loading [11]. But the effect of aqueous corrosion on the fatigue strength with regard to crack initiation in the VHCF regime is not very much studied in literature. In this regime the material is loaded in its elastic domain at the macroscopic scale. In this work the effect of sea water corrosion (under free potential) on the VHCF strength will be studied.

After presenting the investigated material and the experimental conditions both for crack initiation tests and crack propagation tests, experimental results are presented and discussed with regard to the SEM observation of the fracture surface. It is shown that a drastic effect of sea water corrosion decreases the fatigue strength of the steel under sea water flow. The assessment of the crack growth helps us to show that crack initiation dominates the total fatigue life in the gigacycle regime.

Furthermore, additional experiments allow the authors to show experimental evidences of coupling between corrosion and cyclic loading even under ultrasonic loading frequency.

2. Material and experimental conditions

The material studied hereafter is a non-standard hot rolled low alloy steel grade (named R5 according to the International Classification Societies of Off-shore Systems) with a typical fine grain microstructure composed by tempered martensite and bainite as illustrated in [12]. Its chemical composition is shown in Table 1. This steel is used after a double quenching in water at 920°C then 880°C and tempering at 650°C with water cooling. After this heat treatment its mechanical properties are: hardness 317 HB, yield strength 970 MPa, UTS=1018 MPa, Young modulus E=211 GPa. It has to be noticed that this steel is vacuum degassed with low hydrogen content (1 ppm maximum in the liquid steel after the vacuum treatment). Furthermore, very low non-metallic inclusions are present in this steel (see details in [12]).

Table 1: composition of R5 steel (% weight, Fe balance)

C	Mn	Si	P	S	Cr	Ni	Mo	V	O
0.22	1.22	0.3	0.009	0.003	1.07	1.07	0.5	0.09	12

2.1. Fatigue test conditions and specimen geometry

2.1.1. Testing machine and specimen geometry

All the fatigue tests (crack initiation and crack growth) presented hereafter were carried out with an ultrasonic fatigue testing machine [1] operating continuously at 20 kHz (no pulse loading) under fully reversed tension (R= -1) (see [1, 12] for details). Figure 1 shows the dimensions of the two types of specimens used for (i) VHCF crack initiation tests and (ii) fatigue crack growth (FCG) tests. The geometry of the FCG specimens was designed according to the works of Wu [13] and Sun [14]. The crack growth was measured with an optical binocular microscope with a maximum magnification ×200. The roughness of the tested area of the VHCF specimens was Ra=0.6 µm and a few additional specimens with a better roughness (Ra=0.1 µm) were tested too for investigating the effect of roughness. The VHCF specimens were tested under three different conditions: (i) without any corrosion (virgin state), (ii) after pre-corrosion and (iii) under real time artificial sea water flow.

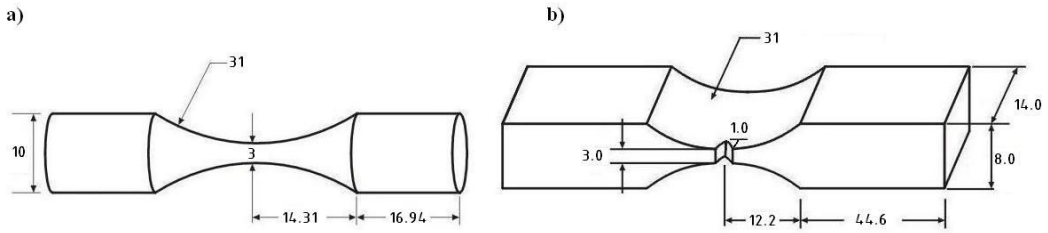

Figure 1: Specimen geometry for (a) VHCF tests, Kt=1.02 in tension, (b) crack growth tests (dimensions in mm).

All the VHCF tests were calibrated by using a wide band (0 to 100 kHz) strain gauge conditioner and a longitudinal strain gauge glued on the specimen surface. Such calibration allows the authors to be certain of the local strain (elastic stress) amplitude and mean value in the narrowest cross section of the specimen. These tests were carried out until a decrease of the resonance frequency of 0.5 kHz that indicates the presence of a macrocrack.

2.1.2. Corrosion of the specimens

The pre-corrosion of the specimens was done according to the ASTM G85 standard: 600 hours in a salt fog corrosion chamber under temperature and humidity control (35°C with 95% of humidity). The salt solution contained 5% of NaCl, its pH was 6.6 and it was applied in the chamber with a

flow rate of 1.52 ml/h. After the pre-corrosion process the specimens were first chemically cleaned and then cleaned with emery paper to remove the oxide layer. Many corrosion pits were created by the salt fog (Figure 2) their diameter is about 30 to 80 µm.

To carry out VHCF tests in sea water environment a special corrosion cell was designed (see [12] for details). To avoid any cavitation it was decided to test the specimens under sea water flow (without immersion). This is representative of the splash zone of the mooring chains. To do that a peristaltic pump creates a flow of sea water (100 ml/min) on two opposite sides of the specimen surface in the tested area (diameter 3 mm). The sea water used was the A3 standard synthetic sea water; its chemical composition in % weight is: 24.53% NaCl, 5.2% MgCl, 4.09% Na_2SO_4, 1.16% Ca_2Cl, 0.695% CaCl and 0.201% $NaHCO_3$. The pH of this solution is 6.6 and no electrical potential was applied between the corrosion solution and the specimens. The temperature of the sea water was 20 – 25°C (room temperature).

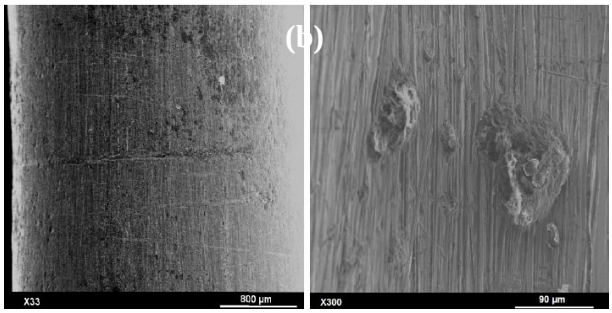

Figure 2: a) Surface of a specimen after pre-corrosion in the salt fog chamber, b) zoom on a corrosion pit.

2.1.3. Fatigue crack growth tests

Fatigue crack growth tests were carried out under fully reversed tension (R=-1) in mode I following a similar methodology than prescribed in ASTM E647 standard. Since with the ultrasonic fatigue testing device the specimen was loaded under displacement control, the range of the stress intensity factor ΔK was computed according to references [13, 14]:

$$\Delta K = U_o \left(\frac{E}{1-\nu^2} \right) \sqrt{\frac{\pi}{a}}\, Y(a/w) \tag{1}$$

with $Y(a/w) = 0.635(a/w) + 1.731(a/w)^2 - 3.979(a/w)^3 + 1.963(a/w)^4$. U_0 is the displacement amplitude imposed at the top of the specimen by the horn of the ultrasonic fatigue testing machine, E is the dynamic modulus and ν is the Poisson ratio of the material, $Y(a/w)$ is a function depending on the specimen geometry, a is the crack length and w is the width of the specimen:

3. Experimental results and discussion

3.1. Fatigue crack initiation tests

Figure 4 shows the S-N curves of the crack initiation tests. A decreasing of around 50 MPa of the fatigue strength for the specimens with pre-corrosion is observed compared to the specimens without any corrosion. The scatter of the fatigue strength of pre-corroded specimens is larger than for virgin ones. There is a drastic effect of sea water flow on the fatigue strength of the R5 steel in the VHCF fatigue regime. Indeed, for the specimens tested under sea water flow, the fatigue strength at 10^7 cycles is around 300 MPa, not far from the value for pre-corroded specimens (360 MPa), but for 3×10^8 cycles the fatigue strength is around 100 MPa only.

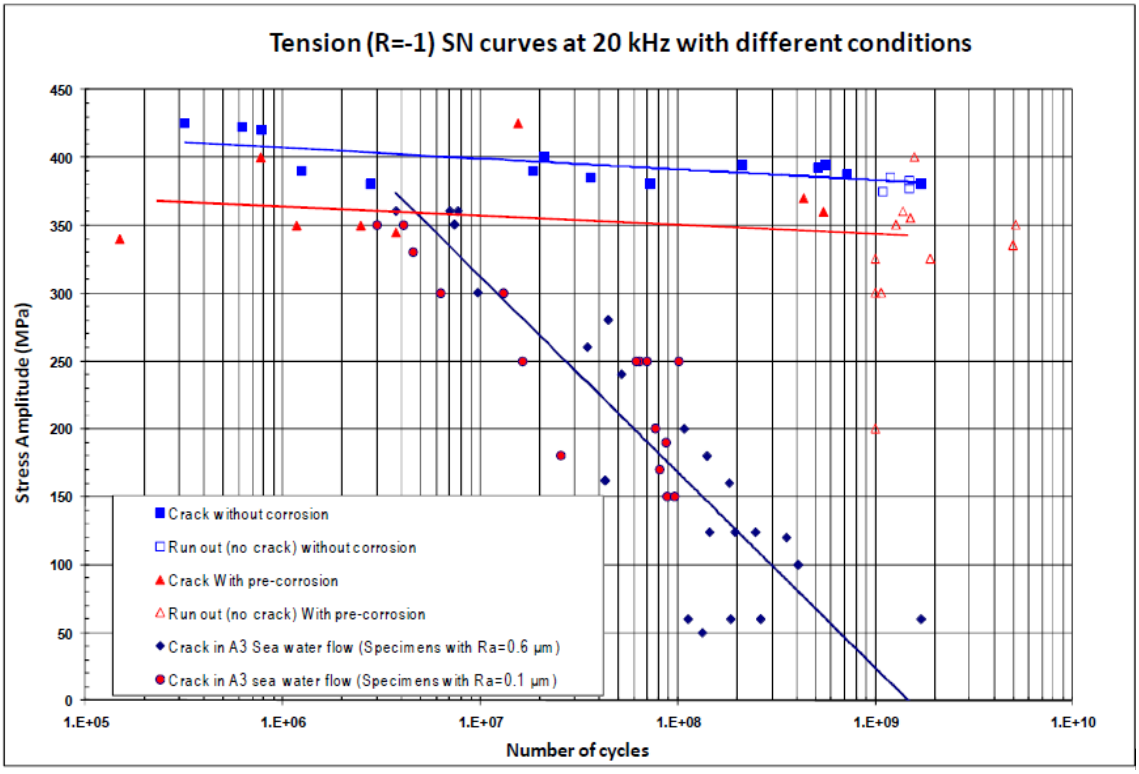

Figure 3: S-N curves of the R5 steel under fully reversed tension at 20 kHz.

The fatigue tests were carried out at 20 kHz under corrosive environment and may be seen first as non representative experiments because of the high loading frequency compared with the characteristic time of the corrosion process. However the results of our experimental data are not so far from the recommendations provided by the International Classification Societies of Off-shore Systems (for design purpose the fatigue strength at 10^8 cycles in sea water should be around 30 MPa). The competition between cyclic loading and corrosion is discussed later in this paper.

3.2. SEM observation of the fracture surfaces

On virgin specimens, even if some unusual internal crack initiations were observed (Figure 5), most of the fatigue cracks initiated at the specimen surface over the cycle range (10^6 – 10^9 cycles). Surface defects were the origin of the cracks for non-corroded specimens and corrosion pits for both pre-corroded specimens and specimens tested under sea water flow (Figures 6 and 7).

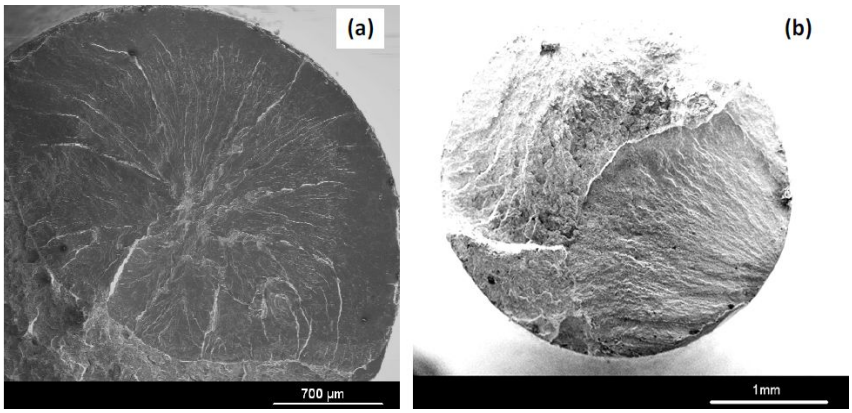

Figure 5: Fracture surface of R5 steel virgin specimens (a) Internal crack initiation σ_a= 380 MPa, N= 2.78×10^6 cycles, (b) surface crack initiation σ_a=395 MPa, N_f =5.61×10^8 cycles.

For the specimens tested under sea water flow the crack initiated all around the specimen surface due to several large corrosion pits. The size of the pits depends on the time (i.e. the number of cycles); their diameter is smaller on the pre-corroded specimens (30 to 80 µm) than under sea water flow (50 to 300 µm) (Figures 6 and 7). Furthermore, a lot of small cracks, perpendicular to the loading direction (mode I), were observed at the surface of the specimen tested under sea water flow (Figure 6C); whereas such small cracks were not observed on both virgin and pre-corroded specimens. This is characteristic of a corrosion/cyclic loading interaction. Since a significant decrease of the fatigue strength has been observed due to corrosion pits (seen as geometrical defects), it is important to determine if the crack propagation dominates or not the total fatigue life compared with the crack initiation phase.

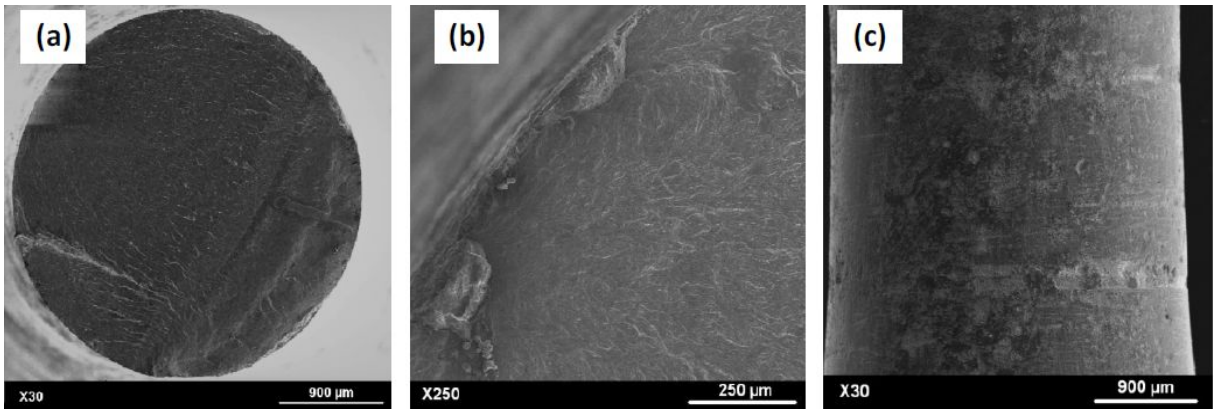

Figure 6: Specimen with pre-corrosion, σ_a=370 MPa, Nf=4.37×10^8 cycles

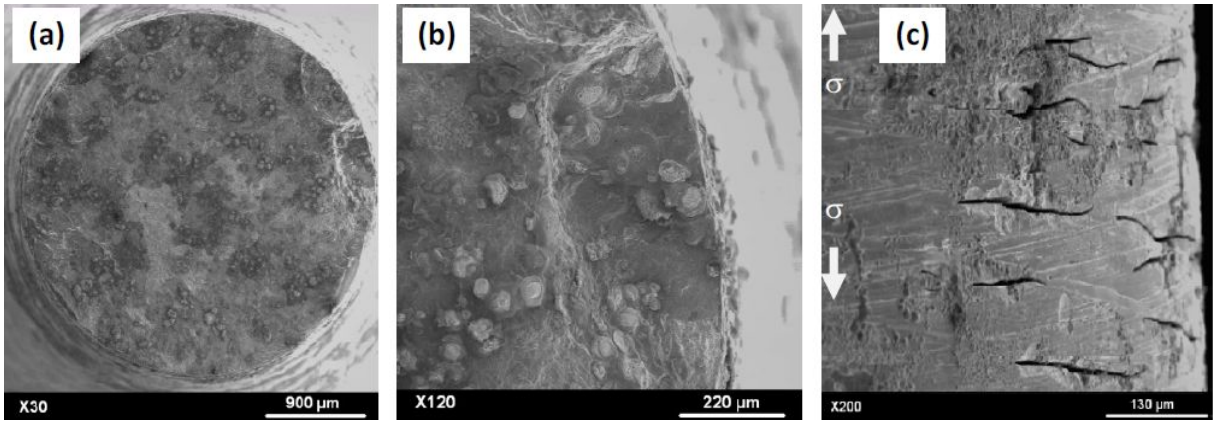

Figure 7: Specimen tested under sea water flow, σ_a=160 MPa, Nf=1.8×10^8 cycles.

4. Assessment of the crack initiation and propagation duration

The experimental $da/dN = f(\Delta K)$ curve for the investigated steel is shown in Figure 9. This shows that in air the mode I (R= –1) stress intensity threshold for R5 steel is around 3.3 MPa√m and as usual the crack growth rate is faster under sea water flow than in air [15]. The fatigue crack propagation duration was assessed according to the work of Paris et al. [8, 9], based on the Paris-Hertzberg-Mc Clintock crack growth model $\frac{da}{dN}=b\left(\frac{\Delta K_{eff}}{E\sqrt{b}}\right)^3$ and $\left(\frac{\Delta K_{eff}}{E\sqrt{b}}\right)=1$ at the corner, where E is the elastic modulus and b is the Burger's vector. The good agreement of this equation with our experimental data and b=0.285 nm was shown in [12]. Since in our experiments at 20 kHz the measurement of K_{op} is not possible, in first approximation $\Delta K_{eff}\approx K_{max}$ was assumed and no water interaction with the stress intensity factor was considered.

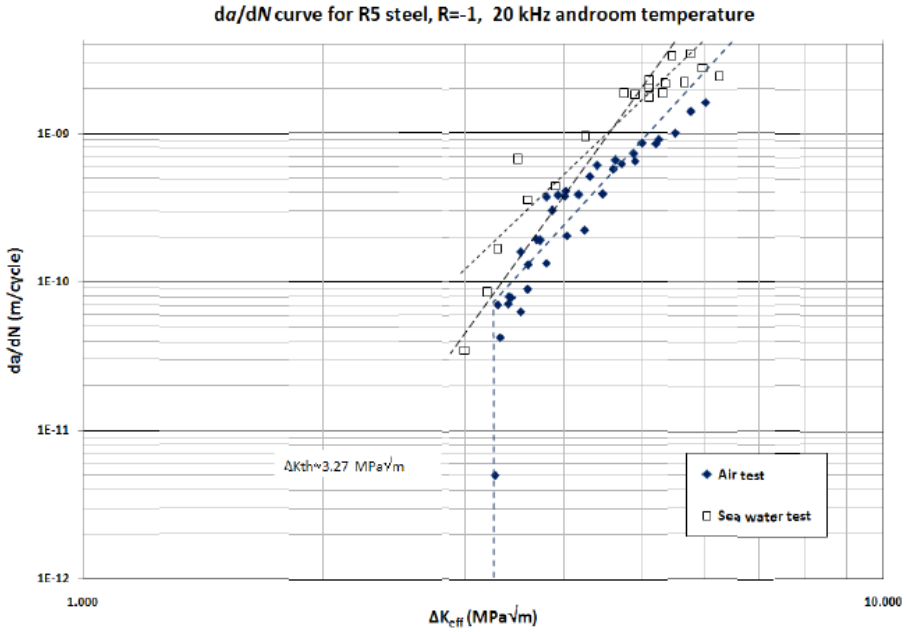

Figure 8: *da/dN =f(ΔK)* curve in mode I for the R5 steel (R= –1), in air and under sea water flow at room temperature.

To assess the duration of the crack propagation phase, a corrosion pit was modeled by a hemispherical surface defect with radius R. The existence of these hemispherical pits was observed by scanning electron microscopy on the surface of different specimens of R5 steel with pre-corrosion in salt fog chamber (Figure 3a) and with corrosion in A3 sea water flow (Figure 7). The longitudinal cross section of a pre-corroded specimen (after 4.37×10^8 cycles under a stress amplitude of 370 MPa) close to the fracture surface was observed as illustrated in Figure 9a. This shows a short crack initiated at a corrosion pit. Based on this observation, an initial fatigue crack of depth a_{int} emanating from the surface of the hemispherical pit and perpendicular to the loading direction due to intercristalline corrosion cracking was assumed. The length of the initial short crack emanating from hemispherical defects was assumed to be a_{int} =10 μm (close to the grain size).

According to the asymptotic approximation proposed by Paris et al [16] the crack tip stress intensity factor in mode I is: $K_I=\sigma Y(x,\nu)\sqrt{\pi a}$, where $x = a/R$, ν is the Poisson ratio, and a function $Y(x,\nu)$ for a penny shape crack emanating from hemispherical surface crack [16] :

$$Y(x/\nu)=1.015\left[A(\nu)+B(\nu)\left(\frac{x}{1+x}\right)+C(\nu)\left(\frac{x}{1+x}\right)^2+D(\nu)\left(\frac{x}{1+x}\right)^3\right](2) \qquad (2)$$

with:

$$A(\nu)=1.683+\frac{3.336}{7-5\nu},B(\nu)=-1.025-\frac{12.3}{7-5\nu},C(\nu)=-1.089+\frac{14.5}{7-5\nu},D(\nu)=1.068-\frac{5.568}{7-5\nu}\ .$$

It was assumed that the propagation of the fatigue crack is divided in three stages: (i) a short crack propagation during $N_{a_{int}-a_0}$ cycles, from initiation a_{int} to the crack size a_0, then (ii) a small crack propagation period $N_{a_0-a_i}$ cycles, from a_0 to the crack size a_i, and (iii) a long crack propagation N_{a_i-a} cycles, from a_i to the final crack size a: $N_{Total}=N_{a_{int}-a_0}+N_{a_0-a_i}+N_{a_i-a}$ .With these three different regimes the very quick propagation of short crack and the quick propagation of small crack compared to long crack were considered.

With these three different regimes [12] the very quick propagation of short crack and the quick propagation of small crack compared to long crack were considered. The detailed equations are given in [12], they were applied to our data assuming that the initial crack has a length, a_0, corresponding to the corner: $da/dN=b$.

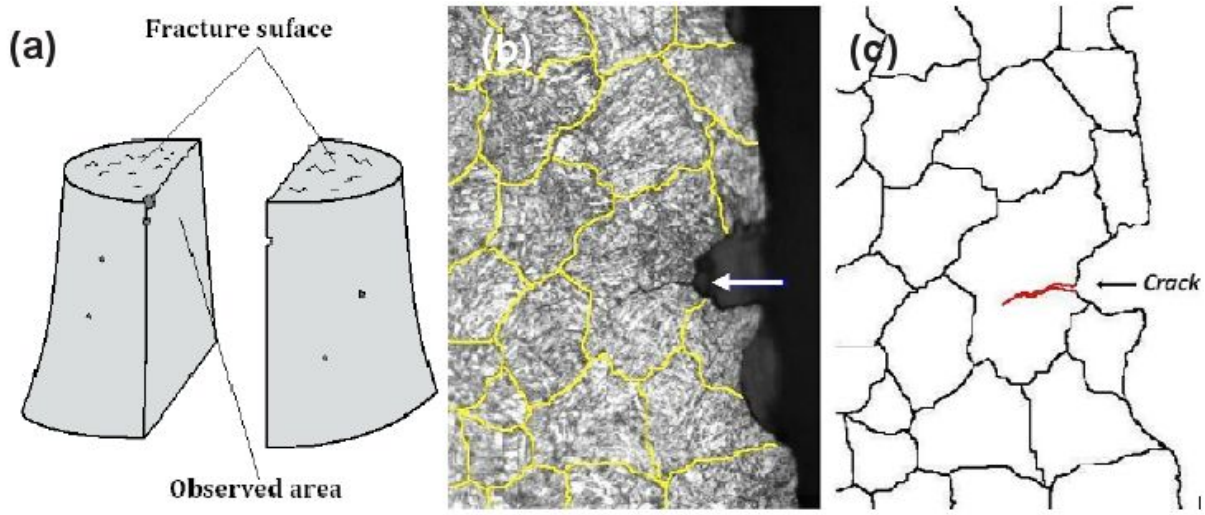

Figure 9: a) Longitudinal cross section of a specimen showing b) a fatigue crack initiation at a corrosion pit and the yellow highlighted old austenitic grains, c) illustration of the short fatigue crack and the grain boundaries.

Two cases are shown in Table 2 with two experimental total fatigue lives N_{exp}; several additional cases are detailed in [12]. In the first case 99.1% of the fatigue life is due to initiation. For the second case, 94% of the fatigue life was consumed by the initiation phase. Furthermore, it has been shown in [12] that with a high value of α and large a_{int}/a_0 one obtains similar N_{Total} results than with a low α and small a_{int}/a_0, that is because with a higher α the crack does not grow as far due to the slope of the da/dN curve in the threshold region, then a_{int}/a_0 must be larger, and with a lower α, a_{int}/a_0 must be smaller.

This calculations show that crack initiation dominates the fatigue life. Even if our calculations were carried out by using the crack growth curve in air, the conclusion is still valid because the crack growth rate for the R5 steel under sea water flow is higher than in air as shown Figure 8 and usually reported in literature [15]. Since the fatigue life is dominated by the crack initiation regime even in corrosive environment, additional experiments have been carried out to try to understand why this initiation period is significantly affected by sea water flow.

5. Additional experiments and discussion about the coupling between cyclic loading and corrosion

To complete these tests an ultrasonic fatigue test has been carried out on a cylindrical specimen. Since during an ultrasonic fatigue test a stationary wave is applied on the specimen, all along this cylinder different stress amplitudes are applied. Figure 9B shows the distribution of the stress amplitude along the cylindrical specimen loaded in its central part with a stress amplitude of 120 MPa (highest value along the specimen). This corresponds to a mean fatigue life of 2×10^8 cycles. For observation, the specimen surface was divided in 13 zones of around 1 cm long, each one was loaded to a specific stress amplitude interval. By testing such a cylinder under sea water flow (Figure 9a), observation of the damaged areas allowed us to investigate the link between the stress amplitude and the damage due to the in-situ fatigue – corrosion process. The specimen failed after 7.37×10^7 cycles.

Case 1: a_0=9.32 µm, σ_a=360 MPa, R=48 µm, a= 2.4 mm, $N_{exp}=5.5\times10^8$ cycles on a pre-corroded specimen				
α	$a$int/a0	$N_{aint\text{-}a0}$	$N_{a0\text{-}ai}$	$N_{ai\text{-}a}$
100	0.9	115,801	44,151	4,507,080
	0.94	13,163		
	0.97	2,300		
Case 2: a_0=41.5 µm, σ_a =160 MPa, R=300 µm, a= 2.6 mm, $N_{exp}=1.83\times10^8$ cycles on specimen tested under sea water flow				
α	$a$int/a0	$N_{aint\text{-}a0}$	$N_{a0\text{-}ai}$	$N_{ai\text{-}a}$
100	0.9	515,466	168,014	10,258,700
	0.94	58,593		
	0.97	10,237		

Table 2: Hemispherical surface crack growth vs. experimental fatigue life, for x=3, and different a_{int}/a_0 ratios.

Microscopic observations of the cylinder surface showed that R5 steel was damaged by fatigue – corrosion in the areas where the stress amplitude was higher than 56 MPa, a few corrosion traces only were observed where the stress amplitude was smaller (Figure 9d). The final fracture occurred where the stress amplitude was between 112 and 120 MPa. This shows an experimental evidence of the coupling between the corrosion process and cyclic loading, even at ultrasonic frequency (20 kHz), since below 56 MPa without any sea water flow there is no failure after 2×10^8 cycles (see the SN curves Figure 3).

Futhermore, three additional tests were carried out on VHCF specimens under the same conditions than all the other tests but, without any cyclic loading. Only the sea water flow was applied on the specimen surface with the same flow rate than for the tests with cyclic loading. The aim of these tests was to quantify the corrosion damage after the same duration than 10^7 cycles (8mn20s at 20 kHz), 10^8 cycles (1h23mn20s at 20 kHz) and 10^9 cycles (13h53mn20s at 20 kHz). No corrosion trace was observed by SEM after 8mn20s. After 1h23mn20s only a few traces of corrosion appear but not pits were observed. Corrosion pits were observed at the specimen surface after 13h53mn20s. The typical size of these pits was varying between 30 and 60 µm (Figure 11) this is significantly smaller than under simultaneous cyclic loading and sea water flow (Figure 8). The same pit size was observed under sea water flow with a stress amplitude of 240 MPa after 5×10^7 cycles. This corresponds to 42 mn only at 20 Khz! This proves that there is a coupling between corrosion and cyclic loading.

Because of such coupling, the question of the roughness effect occurred. Complementary fatigue tests were carried out under sea water flow at a stress amplitude of 250 MPa on the same VHCF specimens but with a polished surface (Ra=0.1 µm) to investigate a possible roughness effect. There was no evidence of the surface roughness effect under sea water flow (Figure 3): the fatigue life is in the scatter band of other experimental data (with Ra=0.6 µm).

This work shows experimental evidence of the coupling between corrosion and cyclic stress, even at 20 kHz while some authors think that fatigue corrosion interaction is not active when the loading frequency is high because of the long characteristic time of the corrosion process compared with the loading period. The observations of this study tend to show that the number of loading cycles (not the time) is a key factor in the fatigue crack initiation phenomenon under sea water flow. This has been recently confirmed by El May et al. [17] on a martensitic stainless steel in NaCl aqueous solution in HCF regime with in-situ fatigue test at around 100 Hz. These authors showed that PSB due to cyclic loading break the passive layer and then corrosion pits appears before crack initiation.

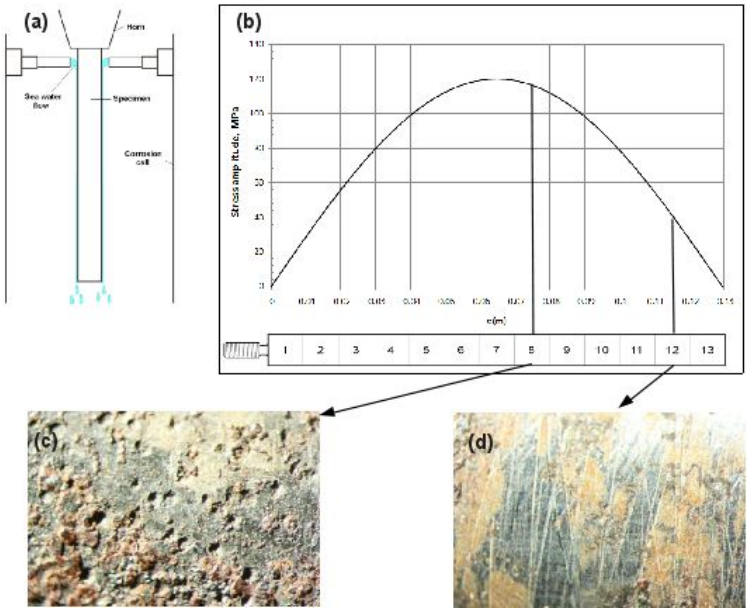

Figure 10: a) schematic illustration of the test principle of a cylindrical specimen with constant cross section under sea water flow, b) evolution of the stress amplitude along the longitudinal axis of the cylindrical specimen for a stress amplitude of 120 MPa in the central cross section, c) and d) optical picture of the specimen surface after 7.37×10^7 cycles in area 8 and area 12 loaded at different stress amplitudes.

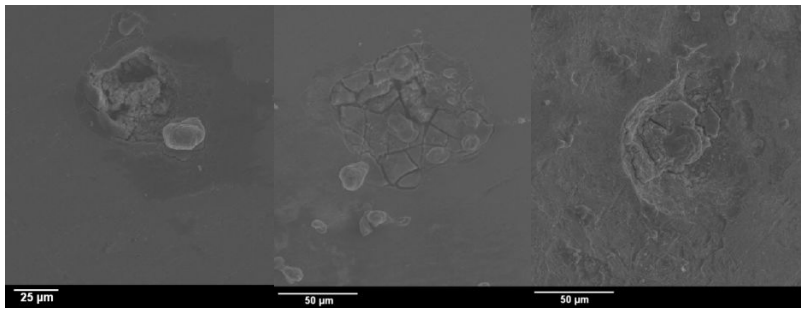

Figure 11: corrosion pits at the surface of a specimen under sea water flow during 13 h 53 min 20 s without any cyclic loading.

Further investigations should be carried out to understand the physical phenomenon involved in the VHCF damage process assisted by corrosion. One may imagine ultrasonic fatigue tests with potentiostatic measurements to monitor corrosion current and potential evolution during a fatigue test. However, not immerged experiments (to avoid cavitation) is a big experimental difficulty for carrying such tests. Investigation of the corrosion pitting kinetics under cyclic loading is probably a key factor for a better understanding of fatigue corrosion process. In situ micro-tomography under both ultrasonic cyclic loading and sea water corrosion may an interesting way for future researches.

6. Conclusion and prospects

Very high cycle fatigue tests were carried out up to 10^9 cycles on smooth specimens in hot rolled martensitic-bainitic steel under three different conditions (i) virgin specimens, (ii) pre-corroded specimens and (iii) under artificial sea water flow during the fatigue test. The fatigue strength at 10^8 cycles is significantly reduced by a factor of 74% compared to the virgin specimens and of 71% compared to the pre-corroded ones. The poor corrosion – fatigue strength is related to the size of the pits. The assessment of the crack growth shows that crack initiation dominates the total fatigue life when $N>10^7$ cycles. A strong coupling between environment and cyclic loading has been proven. Under cyclic loading, even at ultrasonic frequency, fatigue damage and corrosion pitting are interacting for creating crack initiation at very low stress amplitude where no fatigue crack initiates

under fatigue loading alone. This has to be more investigated for understanding the physical mechanisms involved in the corrosion fatigue. Anyway, it has been shown that ultrasonic fatigue test immersed in flowing sea water is a good experimental way to investigate very long life of steel under corrosion conditions with reasonable test time duration.

Acknowledgements

The authors acknowledge both Prof. P.C. Paris for the fruitful discussions about crack propagation modeling and Prof. J-L. Arana for allowing this work and for the financial support of the Vicinay Cadenas company that is thanks too.

References

[1] C. Bathias and P.C. Paris (2005) Gigacycle Fatigue in Mechanical Practice, Marcel Dekker Publisher Co., New York USA.
[2] I. Marines, X. Bin and C. Bathias (2003) An Understanding of very high cycle fatigue of metals, *Int J Fatigue* **25**, 1101-1107.
[3] J.H. Zuo, Z. Wang and H. Han (2008) Effect of microstructure on ultra-high cycle fatigue behavior of Ti-6Al-4V, *Mat Sci Eng* A **473**, 147-152.
[4] H.R. Ammar, A.M. Samuel and F.H. Samuel (2008) Effect of casting imperfections on the fatigue life of 319-F and A356-T6 Al-Si alloys, *Mat Sci Eng* A **473**, 65-75.
[5] H.T. Pang and P.A.S. Reed (2007) Microstructure effects on high temperature fatigue crack initiation and short crack growth in turbine disc nickel-base superalloy Udimet 720 Li, *Mater Sci Eng A* **448**, 67-69.
[6] R.A. Yeske and L.D. Roth (1982) Environmental effects on fatigue of stainless steel at very high frequencies, In: Wells (Westinghouse) J.M. Buck, Roth, Tien (Eds), Ultrasonic fatigue, The Metallurgical Society of AIME, New York, USA, pp. 365–385.
[7] R. Ebara and Y. Yamada (1982) Corrosion fatigue behaviour of 13Cr stainless steel and Ti-6Al-4V at ultrasonic frequency, In: Wells (Westinghouse) J.M. Buck, Roth, Tien (Eds), Ultrasonic fatigue, The Metallurgical Society of AIME, New York, USA, pp. 349–364.
[8] P.C. Paris (2004) The relationship of effective stress intensity, elastic modulus and Burgers-vector on fatigue crack growth as associated with “fish-eye” gigacycle fatigue phenomena, In : *Proceedings of VHCF-3*, Kyoto, Japan, 2004, pp. 1-13.
[9] I. Marines, P.C. Paris, H. Tada and C. Bathias, (2007) Fatigue crack growth from small to long cracks in VHCF with surface initiations, *Int J Fat* **29**, 2072-2078.
[10] E.M. Gutman and G. Soloviof (1996) The mechanochemical behavior of type 316L stainless steel, *Corrosion Science,* **38**, 1141–1145.
[11] T. Pyle, V. Rollins and D. Howard (1975) The influence of cyclic plastic strain on the transient dissolution behavior of 18/8 stainless steel in 3.7M H_2SO_4, *J. Electrochem. Soc.,* **122**, 1445–1453.
[12] T. Palin-Luc, R. Perez-Mora, C. Bathias, G. Dominguez, P.C. Paris and J.L. Arana (2010) Fatigue crack initiation and growth on a steel in the very high cycle fatigue regime with sea water corrosion, *Eng. Fract. Mech.*, **77**, 1953-1962.
[13] T.Y. Wu and C. Bathias (1994) Application of fracture mechanics concepts in ultrasonic fatigue, *Eng Fract Mech,* **47**, 683-690.
[14] Sun (2000) Etude du seuil de fissuration à haute fréquence en fatigue et en fretting fatigue. Ph.D. Thesis, CNAM, Paris France.
[15] C. Bathias and A. Pineau (2010) Fatigue of materials and structures, ISTE Ltd and John Wiley & Sons Inc., 512 p.
[16] P.C. Paris, T. Palin-Luc, H. Tada and N. Saintier (2009) Stresses and crack tip stress intensity factors around spherical and cylindrical voids and inclusions of different elastic properties and with misfit sizes, In Proceedings Int. Crack Path, 8 pages.
[17] M. El May, T. Palin-Luc, N. Saintier and O. Devos (2013) Effect of corrosion on the high cycle fatigue strength of a martensituc stainless steel X12CrNiMoV12-3, *Int. J Fatigue*, **47**, 330–339.